Mixed H_2/H_∞ Tracking Control with Constraints for Single Quadcopter Carrying a Cable-suspended Payload

Minhuan Guo [*] **, Yan Su** [**] **, Dongbing Gu** [***]

[*] *Nanjing University of Science and Technology, Nanjing, 210094, China (e-mail: 312012201@njust.edu.cn).*
[**] *Nanjing University of Science and Technology, Nanjing, 210094, China (suyan@mail.njust.edu.cn).*
[***] *School of Computer Science and Electronic Engineering, University of Essex, Wivenhoe Park, Colchester, CO4 3SQ, UK, (e-mail: dgu@essex.ac.uk)*

Abstract: In order to control a single quadcopter with a cable-suspended payload to follow the desired trajectory, a mixed H_2/H_∞ controller with constraints is developed. Firstly, the Euler-Lagrange dynamic model is built and linearized. Then the extended model for path tracking problem is designed. Based on linear matrix inequality (LMI), state feedback controller H_2 and H_∞ with constraints is illustrated. Aiming to maintain a good balance in transient behaviors and frequency-domain performance, the mixed controller is presented. Finally, the control strategies are utilized in a simulation test and the result validates the proposed method.

Keywords: aircraft control, H_2 norm, H_∞ norm, linear matrix inequality, Lyapunov function, state control.

1. INTRODUCTION

Nowadays unmanned aerial vehicles (UAVs) are gaining more and more popularity in many possible applications including search and rescue, disaster relief operations, environmental monitoring, wireless surveillance networks, and cooperative manipulation. Lifting and transportation of a cable-suspended payload by a quadcopter is a challenging and useful issue.

Much literature has been published around this topic. Cruz and Fierro (2014) addresses the problem of lifting from the ground a cable-suspended load by a quadrotor aerial vehicle, where the mass of the load is unknown. Faust et al. (2013) presents a motion planning method for generating trajectories with minimal residual oscillations for rotorcraft carrying a suspended load and completes the multi-waypoint flight in the cluttered environment. Palunko et al. (2012) uses a high-level planner to provide desired waypoints and utilize a dynamic programming approach to generate the swing-free trajectory to keep the minimum load swing. Sreenath et al. (2013) establishes a differentially-flat hybrid system for the quadrotor-load system and develops a nonlinear geometric controller to enable tracking of outputs. As for the controller design, in De Crousaz et al. (2014), the iLQG method is applied to the hybrid system and the aggressive controller is designed for controlling the payload to pass through a small window. Alothman et al. (2015) proposes a linear quadratic regulator (LQR) for lifting and transporting the load. The single situation is extended to multi-vehicles in Sreenath and Kumar (2013), which addresses the problem of cooperative transportation of a cable-suspended payload by multiple quadcopters.

This paper presents a mixed H_2/H_∞ tracking controller based on linear matrix inequality (LMI). Basically, problems around H_2 and H_∞ control are studied widely. Apkarian et al. (2001), Zhai et al. (2003), and Filasova et al. (2016) describe the framework for H_2 and H_∞ performance based on linear matrix inequality. It is known that while H_∞ control design is mainly concerned with frequency-domain performance, and does not guarantee good transient behaviors for the closed-loop system, H_2 control design gives more suitable performance on system transient behaviors Nonami and Sivrioglu (1996). The proposed method tries to maintain a good balance on transient behavior and frequency-domain performance. Besides, the constraints for the inputs and outputs are also considered in this paper.

The remaining parts of this paper are organized as follows. In section 2, the nonlinear and linear models are described. In section 3, the extended model for tracking problem is given and the mixed H_2/H_∞ controller is presented. In section 4, the proposed method is developed in a simulation test and the results are analyzed. Finally, a brief conclusion is provided.

2. MODEL DESCRIPTION

2.1 System and Notations

The full system is presented in Fig. 1, including the inertial frame, intermediate frame, body-fixed frame, vertical and horizontal forces generated by each propeller and swing

angles of the rope with respect to the intermediate frame. In order to simplify the problem, some reasonable hypotheses are given as follows:

(1) The quadcopter is considered as a symmetrical rigid body.
(2) The payload is considered as a point mass and is attached at the center of the quadcopter.
(3) The cable tension is always non-zero.
(4) The air drag of the propellers is negligible.

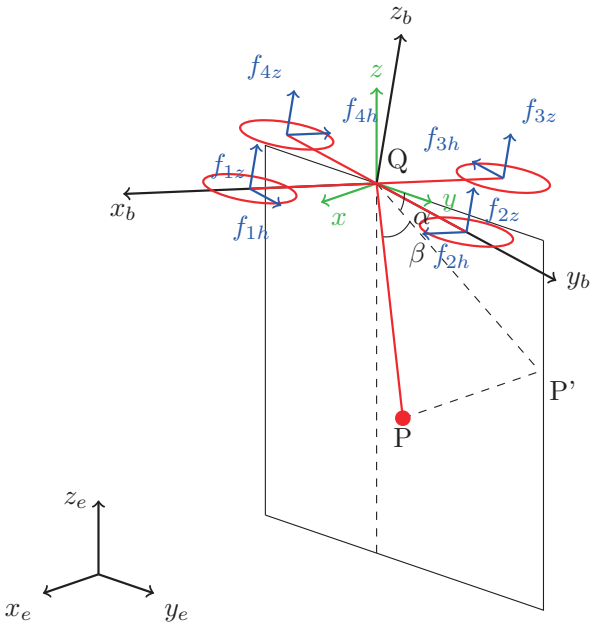

Fig. 1. Single quadcopter with a cable-suspended payload

Partial symbols and acronyms used in this paper are lised in table 1.

Table 1. Symbols and Definitions

Symbol	Description
$\boldsymbol{S_e}: \boldsymbol{x_e y_e z_e}$	Inertial frame
$\boldsymbol{S}: \boldsymbol{xyz}$	Intermediate frame: translate $\boldsymbol{S_e}$ to the center of the quadcopter
$\boldsymbol{S_b}: \boldsymbol{x_b y_b z_b}$	Body-fixed frame
$\boldsymbol{E}_i \in \mathbb{R}^3, i = 1,2,3$	Unit orthogonal vectors of $\boldsymbol{S_e}$
$\boldsymbol{e}_i \in \mathbb{R}^3, i = 1,2,3$	Unit orthogonal vectors of $\boldsymbol{S_b}$
$\boldsymbol{\eta} = [\phi, \theta, \psi]^T \in \mathbb{R}^3$	Euler angles of quadcopter defined in $Z-Y-X$
$\boldsymbol{T}_{e2b} \in \mathbb{R}^{3\times3}$	Transformation matrix from $\boldsymbol{S_e}$ to $\boldsymbol{S_b}$
$\boldsymbol{\Omega} \in \mathbb{R}^3$	Angular velocity of quadcopter in $\boldsymbol{S_b}$
$m_Q = 0.55kg$	Mass of the quadcopter
$m_P = 0.05kg$	Mass of the payload
$\boldsymbol{I}_Q \in \mathbb{R}^3$	Inertial matrix of the quadcopter with respect to $\boldsymbol{S_b}$
$\boldsymbol{\xi}_Q \in \mathbb{R}^3$	Position of the center of quadcopter in $\boldsymbol{S_e}$
$\boldsymbol{\xi}_P \in \mathbb{R}^3$	Position of the payload in $\boldsymbol{S_e}$
$L_r = 0.5m$	Length of the rope
$L_Q = 0.17m$	Length of the quadcopter arm
$\alpha, \beta \in \mathbb{R}$	Angles of the rope with respect to $\boldsymbol{S}$
$\boldsymbol{\rho} \in \mathbb{R}^3$	Unit vector from the payload to the attached point
$\boldsymbol{f}_{iz}, \boldsymbol{f}_{ih} \in \mathbb{R}^3$	Vertial and horizontal forces generated by ith propeller, $i = 1,2,3,4$
$k_F, k_M \in \mathbb{R}$	Propeller aerodynamic parameters

As illustrated in Fig. 1, the following relationships are available.

$$\begin{aligned}
\boldsymbol{\rho} &= [-sin(\beta), -cos(\alpha)cos(\beta), sin(\alpha)cos(\beta)]^T \\
\boldsymbol{\xi}_P &= x_P\boldsymbol{E_1} + y_P\boldsymbol{E_2} + z_P\boldsymbol{E_3} \\
\boldsymbol{\xi}_Q &= \boldsymbol{\xi}_P + L_r\boldsymbol{\rho} \\
\boldsymbol{\Omega} &= \begin{bmatrix} 1 & 0 & -sin(\theta) \\ 0 & cos(\phi) & sin(\phi)cos(\theta) \\ 0 & -sin(\phi) & cos(\phi)cos(\theta) \end{bmatrix} \begin{bmatrix} \dot{\phi} \\ \dot{\theta} \\ \dot{\psi} \end{bmatrix}
\end{aligned} \tag{1}$$

2.2 Euler-Lagrange Modeling

The quadcopter-payload system has 8 degrees of freedom. Choosing $\boldsymbol{q} = [x_P, y_P, z_P, \alpha, \beta, \phi, \theta, \psi]^T$ as the generalized coordinates will not only be convenient while controlling the trajectory of the payload but also be helpful for extending to multi-vehicle situation. As a result, the Lagrangian is given by

$$\begin{aligned}
T &= \frac{1}{2}m_P\dot{\boldsymbol{\xi}}_P^T \cdot \dot{\boldsymbol{\xi}}_P + \frac{1}{2}m_Q\dot{\boldsymbol{\xi}}_Q^T \cdot \dot{\boldsymbol{\xi}}_Q + \frac{1}{2}\boldsymbol{\Omega}^T\boldsymbol{I}_Q\boldsymbol{\Omega} \\
U &= m_P g\boldsymbol{\xi}_P \cdot \boldsymbol{E}_3 + m_Q g\boldsymbol{\xi}_Q \cdot \boldsymbol{E}_3 \\
L &= T - U
\end{aligned} \tag{2}$$

Then the Euler-Lagrange equation is

$$\frac{d}{\mathrm{dt}}\left(\frac{\partial L}{\partial \dot{\boldsymbol{q}}}\right) - \frac{\partial L}{\partial \boldsymbol{q}} = \boldsymbol{Q} \tag{3}$$

The generalized forces $\boldsymbol{Q}$ defined here are based on the choice of the generalized coordinates $\boldsymbol{q}$ and the external conservative forces $\sum \boldsymbol{F}_i$. The force $\boldsymbol{F}_i$ consists of two complements $\boldsymbol{f}_{iz}$ and $\boldsymbol{f}_{ih}$ (equation (4)) which are related with the angular speed ω_i of ith propeller.

$$\begin{aligned}
\boldsymbol{F}_i &= \boldsymbol{f}_{iz} + \boldsymbol{f}_{ih}, i = 1,2,3,4 \\
\boldsymbol{f}_{iz} &= k_F\omega_i^2\boldsymbol{e}_3, i = 1,2,3,4 \\
\boldsymbol{f}_{1h} &= k_M\omega_1^2\boldsymbol{e}_2 \\
\boldsymbol{f}_{2h} &= k_M\omega_2^2\boldsymbol{e}_1 \\
\boldsymbol{f}_{3h} &= -k_M\omega_3^2\boldsymbol{e}_2 \\
\boldsymbol{f}_{4h} &= -k_M\omega_4^2\boldsymbol{e}_1
\end{aligned} \tag{4}$$

where $\boldsymbol{e}_i = \boldsymbol{T}_{e2b}\boldsymbol{E}_i$, $i = 1,2,3$.

As seen in Fig. 1, the point where the force $\boldsymbol{F}_i$ is applied on is the center of each propeller and the corresponding position vector is noted as $\boldsymbol{\xi}_i$ seen in equation (5).

$$\begin{aligned}
\boldsymbol{\xi}_1 &= \boldsymbol{\xi}_Q + L_Q\boldsymbol{e}_1 \\
\boldsymbol{\xi}_2 &= \boldsymbol{\xi}_Q + L_Q\boldsymbol{e}_2 \\
\boldsymbol{\xi}_3 &= \boldsymbol{\xi}_Q - L_Q\boldsymbol{e}_1 \\
\boldsymbol{\xi}_4 &= \boldsymbol{\xi}_Q - L_Q\boldsymbol{e}_2
\end{aligned} \tag{5}$$

According to the principle of virtual work, the generalized forces are given by equation (6).

$$Q_i = \sum_{j=1}^{4} \frac{\partial(\boldsymbol{F}_j \cdot \boldsymbol{\xi}_j)}{\partial q_i}, i = 1,2,..,8 \tag{6}$$

Taking the generalized forces (detailed in (A.1)) and equation (2) into equation (3), the Euler-Lagrange equation can be rewritten in

$$\boldsymbol{M}\ddot{\boldsymbol{q}} = f(\boldsymbol{q}, \dot{\boldsymbol{q}}) \tag{7}$$

where $\boldsymbol{M}$ and $f(\boldsymbol{q}, \dot{\boldsymbol{q}})$ are detailed in (A.2) and (A.3) respectively.

Considering the balance situation as the equilibrium point ($\boldsymbol{x}_0$,$\boldsymbol{u}_0$), the linearized model is obtained in equation (8).

$$\ddot{\boldsymbol{q}} = \boldsymbol{M}^{-1}\frac{\partial f}{\partial \boldsymbol{x}}\bigg|_{\boldsymbol{x}_0}\Delta\boldsymbol{x} + \boldsymbol{M}^{-1}\frac{\partial f}{\partial \boldsymbol{u}}\bigg|_{\boldsymbol{u}_0}\Delta\boldsymbol{u} \tag{8}$$

Furthermore, equation (8) can be stated in the following standard state-space form.

$$\begin{aligned}\dot{\boldsymbol{x}} &= \boldsymbol{A}\boldsymbol{x} + \boldsymbol{B}\boldsymbol{u}\\ \boldsymbol{y} &= \boldsymbol{C}\boldsymbol{x}\end{aligned} \tag{9}$$

where $\boldsymbol{A} \in \mathbb{R}^{16\times16}$ and $\boldsymbol{B} \in \mathbb{R}^{16\times4}$ are detailed in(A.4) and (A.5), $\boldsymbol{C} = \boldsymbol{I}^{16\times16}$.

$\boldsymbol{x} = \left[x_P, \dot{x}_P, y_P, \dot{y}_P, z_P, \dot{z}_P, \alpha, \dot{\alpha}, \beta, \dot{\beta}, \phi, \dot{\phi}, \theta, \dot{\theta}, \psi, \dot{\psi}\right]^T \in \mathbb{R}^{16}$, $\boldsymbol{u} = [\omega_1, \omega_2, \omega_3, \omega_4]^T \in \mathbb{R}^4, \boldsymbol{y} \in \mathbb{R}^{16}$

3. CONTROL STRATEGIES

3.1 Extended Model for Tracking Path

Taking account of the integrations of the position tracking error, the diagram of state feedback controller is seen in Fig. 2.

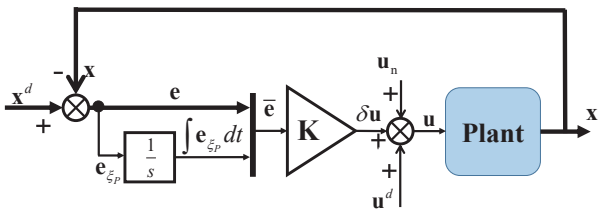

Fig. 2. Diagram of extended state feedback controller

The desired and feasible trajectory is $\left(\boldsymbol{x}^d, \boldsymbol{u}^d\right)$, so the state error is $\boldsymbol{e} \in \mathbb{R}^{16} := \boldsymbol{x}^d - \boldsymbol{x}$.

The integration of the position error is $\int \boldsymbol{e}_{\xi_P} dt \in \mathbb{R}^3$.

The new error state is $\bar{\boldsymbol{e}} = \left[\boldsymbol{e}^T, \int \boldsymbol{e}_{\xi_P}^T dt\right]^T \in \mathbb{R}^{19}$.

Therefore, equation (9) can be stated in following form of tracking error $\bar{\boldsymbol{e}}$ and disturbance inputs $\boldsymbol{w} = \boldsymbol{u}_n \in \mathbb{R}^4$.

$$\dot{\bar{\boldsymbol{e}}} = \bar{\boldsymbol{A}}\bar{\boldsymbol{e}} + \boldsymbol{B}_\omega\boldsymbol{w} + \boldsymbol{B}_u\boldsymbol{\delta u} \tag{10}$$

where, $\bar{\boldsymbol{A}} = \left[\begin{array}{c|c}\boldsymbol{A} & \boldsymbol{0}\\ \hline \boldsymbol{F} & \boldsymbol{0}\end{array}\right] \in \mathbb{R}^{19\times19}, \boldsymbol{F} = \boldsymbol{B}_\omega = \begin{bmatrix}\boldsymbol{B}\\ \boldsymbol{0}\end{bmatrix} \in \mathbb{R}^{19\times4}, \boldsymbol{B}_u = \begin{bmatrix}\boldsymbol{B}\\ \boldsymbol{0}\end{bmatrix} \in \mathbb{R}^{19\times4}$. All the states are detectable and considered as measurement outputs. The H_2, H_∞ and constraint performance outputs are as follows:

$$\begin{aligned}\boldsymbol{z}_2 &= \boldsymbol{C}_2\boldsymbol{x} + \boldsymbol{D}_2\boldsymbol{u}\\ \boldsymbol{z}_\infty &= \boldsymbol{C}_\infty\boldsymbol{x} + \boldsymbol{D}_\infty\boldsymbol{u}\\ \boldsymbol{z}_c &= \boldsymbol{C}_c\boldsymbol{x} + \boldsymbol{D}_c\boldsymbol{u}\end{aligned} \tag{11}$$

where $\boldsymbol{C}_2$, $\boldsymbol{D}_2$, $\boldsymbol{C}_\infty$, $\boldsymbol{D}_\infty$, $\boldsymbol{C}_c$, $\boldsymbol{D}_c$ are appropriate weight matrix.

As a result, equation (11) is equal to the following transfer function matrix in terms of H_2 and H_∞ performances.

$$\boldsymbol{G} = \begin{bmatrix}\boldsymbol{G}_{11} & \boldsymbol{G}_{12}\\ \boldsymbol{G}_{21} & \boldsymbol{G}_{22}\end{bmatrix} = \left[\begin{array}{c|cc}\bar{\boldsymbol{A}} & \boldsymbol{B}_w & \boldsymbol{B}_u\\ \hline \boldsymbol{C}_2 & 0 & \boldsymbol{D}_2\\ \boldsymbol{C}_\infty & 0 & \boldsymbol{D}_\infty\end{array}\right] \tag{12}$$

The problem of mixed H_2/H_∞ tracking control with constraints is described like:

$$\begin{aligned}&\min_{K_{mix}} \|\boldsymbol{T}_{z2u}(\boldsymbol{K}_{mix})\|_2\\ &s.t.\|\boldsymbol{T}_{z\infty w}(\boldsymbol{K}_{mix})\|_\infty \le \gamma\\ &|\boldsymbol{u}_i(t)| \le u_{i\max}\\ &|\boldsymbol{z}_{ci}(t)| \le z_{i\max}\end{aligned} \tag{13}$$

where, γ is the acceptable gain of H_∞ norm, $u_{i\max}$ and $z_{i\max}$ are the maximum constraints. Then the feedback controller is:

$$\boldsymbol{u} = \boldsymbol{\delta u} + \boldsymbol{u}^d = \boldsymbol{K}_{mix}\bar{\boldsymbol{e}} + \boldsymbol{u}^d \tag{14}$$

3.2 Mixed H_2/H_∞ LMI Control with Constraints

Lemma 1. (H_2 Performance)
Given an upper bound $\lambda > 0$, if there exist symmetric positive definite matrices $\boldsymbol{X}_2$, $\boldsymbol{Z}$ and general matrix $\boldsymbol{R}_2$ satisfying

$$\begin{aligned}\boldsymbol{X}_2 = \boldsymbol{X}_2^T \succ 0, \boldsymbol{Z} = \boldsymbol{Z}^T \succ 0\\ \begin{bmatrix}\boldsymbol{A}\boldsymbol{X}_2 + \boldsymbol{X}_2\boldsymbol{A}^T + \boldsymbol{B}_u\boldsymbol{R}_2 + \boldsymbol{R}_2^T\boldsymbol{B}_u^T & *\\ \boldsymbol{B}_u^T & -\boldsymbol{I}\end{bmatrix} \succ 0\\ \begin{bmatrix}\boldsymbol{Z} & *\\ \boldsymbol{X}_2\boldsymbol{C}_2^T + \boldsymbol{R}_2^T\boldsymbol{D}_2^T & \boldsymbol{X}_2\end{bmatrix} \succ 0\\ tr\boldsymbol{Z} < \lambda^2\end{aligned} \tag{15}$$

where state-feedback gain matrix $\boldsymbol{K}_2 = \boldsymbol{R}_2\boldsymbol{X}_2^{-1}$. Then, the controller stabilizes the closed-loop system and the upper bound of H_2 performance index is λ.

Proof. See Apkarian et al. (2001).

Lemma 2. (H_∞ Performance with Constraints)
Given an upper bound $\gamma > 0$, if there exit symmetric positive definite matrix $\boldsymbol{Q}_\infty$, positive diagonal matrix $\boldsymbol{U}, \boldsymbol{Y}$ and general matrix $\boldsymbol{Y}_\infty$ satisfying

$$\begin{aligned}\boldsymbol{Q}_\infty = \boldsymbol{Q}_\infty^T \succ 0\\ \begin{bmatrix}\boldsymbol{A}\boldsymbol{Q}_\infty + \boldsymbol{Q}_\infty\boldsymbol{A}^T + \boldsymbol{B}_u\boldsymbol{Y}_\infty + \boldsymbol{Y}_\infty^T\boldsymbol{B}_u^T & * & *\\ \boldsymbol{C}_\infty\boldsymbol{Q}_\infty + \boldsymbol{D}_\infty\boldsymbol{Y}_\infty & -\gamma\boldsymbol{I} & *\\ \boldsymbol{B}_w^T & \boldsymbol{0} & -\gamma\boldsymbol{I}\end{bmatrix} \prec 0\\ \begin{bmatrix}\frac{1}{\alpha}\boldsymbol{U} & \boldsymbol{Y}_\infty\\ * & \boldsymbol{Q}_\infty\end{bmatrix} \succ 0, \boldsymbol{U}_{ii} \prec u_{imax}^2\\ \begin{bmatrix}\frac{1}{\alpha}\boldsymbol{Y} & \boldsymbol{C}_c\boldsymbol{Q}_\infty + \boldsymbol{D}_c\boldsymbol{Y}_\infty\\ * & \boldsymbol{Q}_\infty\end{bmatrix} \succ 0, \boldsymbol{Y}_{ii} \prec z_{imax}^2\end{aligned} \tag{16}$$

where state-feedback gain matrix $\boldsymbol{K}_\infty = \boldsymbol{Y}_\infty \boldsymbol{Q}_\infty^{-1}$. Then, the controller meets the constraints, robustly stabilizes the closed-loop system and the upper bound of H_∞ performance index is γ.

Proof. The proof for H_∞ is seen in Filasova et al. (2016). Since $\boldsymbol{K}_\infty = \boldsymbol{Y}_\infty \boldsymbol{Q}_\infty^{-1}$ is the state feedback gain for H_∞ performance, it guarantees the closed system $\boldsymbol{A} + \boldsymbol{B}_u \boldsymbol{K}_\infty$ to be asymptotic stable.

Choosing $V(\boldsymbol{x}(t)) = ||\boldsymbol{Q}_\infty^{-1/2} \boldsymbol{x}(t)||_2^2$ as the Lyapunov function, we get

$$\frac{d}{dt} V(\boldsymbol{x}(t)) + \gamma^{-1} \|\boldsymbol{z}_\infty(t)\|^2 - \gamma \|\boldsymbol{w}(t)\|^2 \leq 0 \tag{17}$$

After integration,

$$V(\boldsymbol{x}(t)) + \gamma^{-1} \int_0^t \|\boldsymbol{z}_\infty(\tau)\|^2 d\tau \leq \gamma \int_0^t \|\boldsymbol{w}(\tau)\|^2 d\tau + V(\boldsymbol{x}(0)) \tag{18}$$

Assume $\int_0^\infty \|\boldsymbol{w}(t)\|^2 dt \leq w_{\max}$, equation (17) means the state stays in the ellipsoid:

$$\Omega(\boldsymbol{Q}_\infty^{-1/2}, \alpha) = \{\boldsymbol{x} \in \mathbb{R}^n | V(\boldsymbol{x}) \leq \alpha\} \tag{19}$$

where, $\alpha = \gamma w_{\max} + V(\boldsymbol{x}(0))$.

Constraints for the inputs and outputs are:

$$\begin{aligned}
\max_{t \geq 0} |\boldsymbol{u}_i(t)|^2 &= \max |(\boldsymbol{Y}_\infty \boldsymbol{Q}_\infty^{-1})_i \boldsymbol{x}(t)|^2 \\
&\leq \max_{\boldsymbol{x} \in \Omega} |(\boldsymbol{Y}_\infty \boldsymbol{Q}_\infty^{-1})_i \boldsymbol{x}|^2 \\
&\leq \alpha ||(\boldsymbol{Y}_\infty \boldsymbol{Q}_\infty^{-\frac{1}{2}})_i||_2^2 \\
\max_{t \geq 0} |\boldsymbol{z}_{ci}(t)|^2 &= \max |(\boldsymbol{C}_c + \boldsymbol{D}_c \boldsymbol{Y}_\infty \boldsymbol{Q}_\infty^{-1})_i \boldsymbol{x}(t)|^2 \\
&\leq \max_{\boldsymbol{x} \in \Omega} |(\boldsymbol{C}_c + \boldsymbol{D}_c \boldsymbol{Y}_\infty \boldsymbol{Q}_\infty^{-1})_i \boldsymbol{x}|^2 \\
&\leq \alpha ||((\boldsymbol{C}_c \boldsymbol{Q}_\infty + \boldsymbol{D}_c \boldsymbol{Y}_\infty) \boldsymbol{Q}_\infty^{-\frac{1}{2}})_i||_2^2
\end{aligned} \tag{20}$$

where, subscript i means the ith row of the matrix.

Finally, equation (20) can be rewritten in the forms in equation (16). This concludes the proof.

Lemma 3. (H_2/H_∞ Performance with Constraints) Given upper bounds of H_2 and H_∞ are λ and γ respectively, if there exist symmetric positive definite matrices $\boldsymbol{X}$, $\boldsymbol{Z}$, positive diagonal matrix $\boldsymbol{U}, \boldsymbol{Y}$ and general matrix $\boldsymbol{R}$ satisfying

$$\begin{aligned}
\boldsymbol{X} = \boldsymbol{X}^T \succ 0, \boldsymbol{Z} = \boldsymbol{Z}^T \succ 0 \\
tr \boldsymbol{Z} < \lambda^2 \\
\begin{bmatrix} \boldsymbol{Z} & * \\ \boldsymbol{X}\boldsymbol{C}_2^T + \boldsymbol{R}^T \boldsymbol{D}_2^T & \boldsymbol{X} \end{bmatrix} \succ 0 \\
\begin{bmatrix} \boldsymbol{A}\boldsymbol{X} + \boldsymbol{X}\boldsymbol{A}^T + \boldsymbol{B}_u \boldsymbol{R} + \boldsymbol{R}^T \boldsymbol{B}_u^T & * \\ \boldsymbol{B}_u^T & -\boldsymbol{I} \end{bmatrix} \succ 0 \\
\begin{bmatrix} \boldsymbol{A}\boldsymbol{X} + \boldsymbol{X}\boldsymbol{A}^T + \boldsymbol{B}_u \boldsymbol{R} + \boldsymbol{R}^T \boldsymbol{B}_u^T & * & * \\ \boldsymbol{C}_\infty \boldsymbol{X} + \boldsymbol{D}_\infty \boldsymbol{R} & -\gamma \boldsymbol{I} & * \\ \boldsymbol{B}_w^T & \boldsymbol{0} & -\gamma \boldsymbol{I} \end{bmatrix} \prec 0 \\
\begin{bmatrix} \frac{1}{\alpha} \boldsymbol{U} & \boldsymbol{R} \\ * & \boldsymbol{X} \end{bmatrix} \succ 0, \boldsymbol{U}_{ii} \prec u_{imax}^2 \\
\begin{bmatrix} \frac{1}{\alpha} \boldsymbol{Y} & \boldsymbol{C}_c \boldsymbol{X} + \boldsymbol{D}_c \boldsymbol{R} \\ * & \boldsymbol{X} \end{bmatrix} \succ 0, \boldsymbol{Y}_{ii} \prec z_{imax}^2
\end{aligned} \tag{21}$$

where state-feedback gain matrix $\boldsymbol{K}_{mix} = \boldsymbol{R}\boldsymbol{X}^{-1}$. Then, the controller meets the constraints, robustly stabilizes the closed-loop system and the upper bound of H_∞ performance index is γ and stabilizes the closed-loop system and the upper bound of H_2 performance index is λ.

Proof. Considering that $\boldsymbol{K}$ in Lemma 1 and 2 should be consistent, after assuming $\boldsymbol{X} = \boldsymbol{X}_2 = \boldsymbol{Q}_\infty$ and $\boldsymbol{R} = \boldsymbol{R}_2 = \boldsymbol{Y}_\infty$, equation (21) is obtained.

4. SIMULATION RESULTS

In order to check the effectiveness of the proposed controller, a simulation test has been implemented on Matlab/Simulink. Specifically, the designed controllers try to carry the payload from the initial position $(0, 0, 0)$ to the desired position $(-1, 1, 1.0)$. The test results are seen in Fig. 3-7.

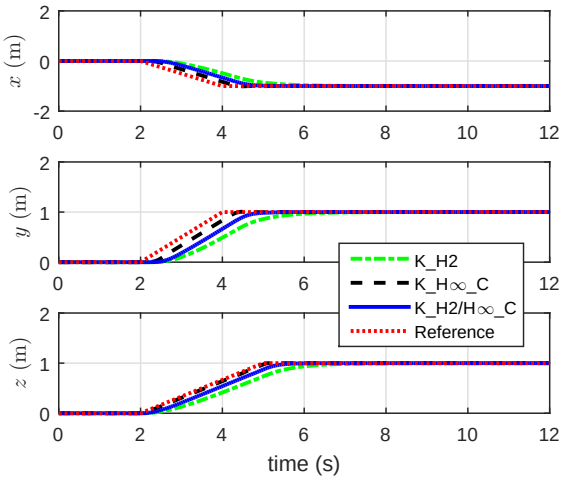

Fig. 3. Position of the payload

As for the trajectory tracking performance in Fig. 3, H_2 controller has the longest response time, whilst H_∞ and H_{mix} have a shorter and nearly close one.

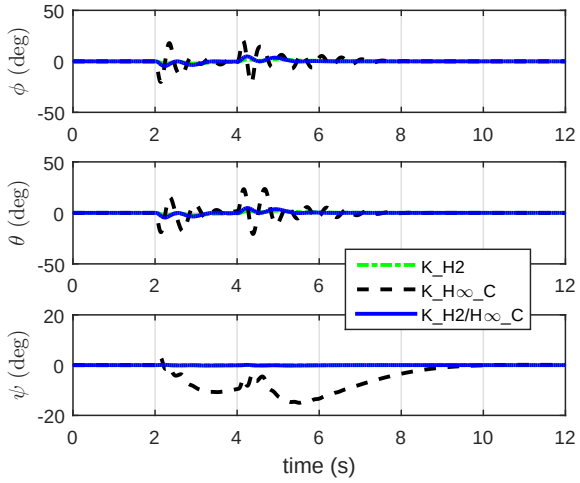

Fig. 4. Attitude of the quadcopter

In terms of the quadcopter's attitude (Fig. 4), H_2 has the most stable angular rate and H_∞ has the worst

performance. In comparison, H_{mix} is much smoother than H_∞ and a little greater than H_2.

Considering the inertia of the payload, the swing angles (α and β) will not change dramatically. Seen in Fig. 5, H_∞ and H_{mix} have larger but acceptable swing angles since they have a shorter response time for trajectory tracking problem.

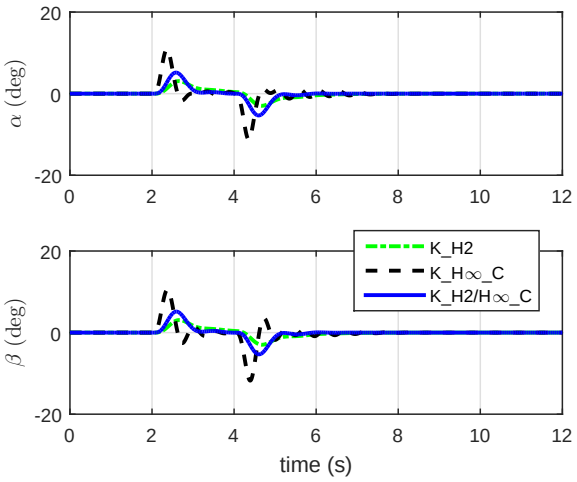

Fig. 5. Swing angles of the cable

Fig. 6 and 7 illustrate the H_2 and H_∞ norm performance for these three controllers. It is obvious that H_{mix} maintains a balance on transient behavior and frequency domain performance.

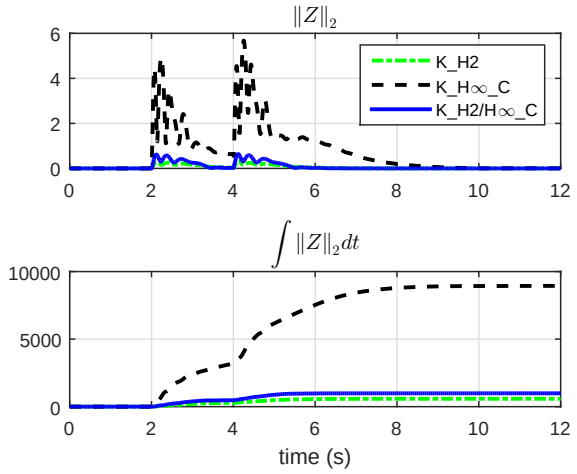

Fig. 6. H_2 performance

In Fig. 6, when the quadcotor starts to carry the payload to the desired position, the H_∞ controller causes too much oscillation which is bad for maintaining stable. However, H_{mix} does betther in eliminating these side effects.

In Fig. 7, H_{mix} and H_∞ have nearly the same and the smallest singular values in the low-frequency area which means they have a strong ability to track the desired trajectory.

Apart from the step response test, another simulation video for controlling the payload to track a star shape trajectory is available at `https://www.youtube.com/watch?v=zpD9ROTo-2Y\&feature=youtu.be`.

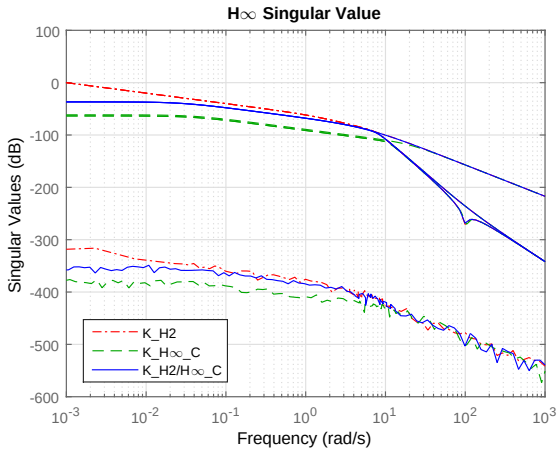

Fig. 7. Singular values of the transfer function matrix from $\boldsymbol{w}$ to $\boldsymbol{Z}_\infty$

In conclusion, it is in contradiction that trying to both increase the ability for trajectory tracking and keep the quadcopter stable. Basically, the proposed H_{mix} method utilizes H_∞ for path tracking and H_2 for attitude regulation. The results have been validated in the simulation test.

5. CONCLUSION

This paper presents a mixed H_2/H_∞ controller with constraints for single quadcopter with a cable-suspended payload. The simulation results show that the proposed controller efficiently eliminates the position error and still keeps a smooth change for the quadcopter's attitude. The future work is to utilize this approach for practical situation together with trajectory planning.

REFERENCES

Yaser Alothman, Wesam Jasim, and Dongbing Gu. Quadrotor lifting-transporting cable-suspended payloads control. In *Automation and Computing (ICAC), 2015 21st International Conference on*, pages 1–6. IEEE, 2015.

Pierre Apkarian, Hoang Duong Tuan, and Jacques Bernussou. Continuous-time analysis, eigenstructure assignment, and h 2 synthesis with enhanced linear matrix inequalities (lmi) characterizations. *IEEE Transactions on Automatic Control*, 46(12):1941–1946, 2001.

Patricio Cruz and Rafael Fierro. Autonomous lift of a cable-suspended load by an unmanned aerial robot. In *2014 IEEE Conference on Control Applications (CCA)*, pages 802–807. IEEE, 2014.

Cedric De Crousaz, Farbod Farshidian, and Jonas Buchli. Aggressive optimal control for agile flight with a slung load. In *IROS 2014 Workshop on Machine Learning in Planning and Control of Robot Motion*. Citeseer, 2014.

Aleksandra Faust, Ivana Palunko, Patricio Cruz, Rafael Fierro, and Lydia Tapia. Learning swing-free trajectories for uavs with a suspended load. In *Robotics and*

Automation (ICRA), 2013 IEEE International Conference on, pages 4902–4909. IEEE, 2013.

Anna Filasova et al. On enhanced mixed $h2/h\infty$ design conditions for control of linear time-invariant systems. In *Carpathian Control Conference (ICCC), 2016 17th International*, pages 384–389. IEEE, 2016.

Kenzo Nonami and SELIM Sivrioglu. Active vibration control using lmi-based mixed $h2/h\infty$ state and output feedback control with nonlinearity. In *Decision and Control, 1996., Proceedings of the 35th IEEE Conference on*, volume 1, pages 161–166. IEEE, 1996.

Ivana Palunko, Rafael Fierro, and Patricio Cruz. Trajectory generation for swing-free maneuvers of a quadrotor with suspended payload: A dynamic programming approach. In *Robotics and Automation (ICRA), 2012 IEEE International Conference on*, pages 2691–2697. IEEE, 2012.

Koushil Sreenath and Vijay Kumar. Dynamics, control and planning for cooperative manipulation of payloads suspended by cables from multiple quadrotor robots. *rn*, 1(r2):r3, 2013.

Koushil Sreenath, Taeyoung Lee, and Vijay Kumar. Geometric control and differential flatness of a quadrotor uav with a cable-suspended load. In *52nd IEEE Conference on Decision and Control*, pages 2269–2274. IEEE, 2013.

Guisheng Zhai, Shinichi Murao, Naoki Koyama, and Masaharu Yoshida. Low order h controller design: An lmi approach. In *European Control Conference (ECC), 2003*, pages 3070–3075. IEEE, 2003.

Appendix A. SOME RESULTS

Generalized forces:

$$
\begin{aligned}
Q_1 =& k_M(\omega_2^2-\omega_4^2)C\theta C\psi + C\phi(k_F(\omega_1^2+\omega_2^2+\omega_3^2+\omega_4^2)C\psi S\theta \\
&+ k_M(-\omega_1^2+\omega_3^2)S\psi) + S\phi(k_M(\omega_1^2-\omega_3^2)C\psi S\theta + k_F(\omega_1^2+\omega_2^2+\omega_3^2+\omega_4^2)S\psi)\\
Q_2 =& -k_F(\omega_1^2+\omega_2^2+\omega_3^2+\omega_4^2)C\psi S\phi + k_M((\omega_2^2-\omega_4^2)C\theta + (\omega_1^2-\omega_3^2)S\theta S\phi)S\psi \\
&+ C\phi(k_M(\omega_1^2-\omega_3^2)C\psi + k_F(\omega_1^2+\omega_2^2+\omega_3^2+\omega_4^2)S\theta S\psi)\\
Q_3 =& k_M(-\omega_2^2+\omega_4^2)S\theta + C\theta(k_F(\omega_1^2+\omega_2^2+\omega_3^2+\omega_4^2)C\phi + k_M(\omega_1^2-\omega_3^2)S\phi)\\
Q_4 =& L_r(S\alpha(-k_F(\omega_1^2+\omega_2^2+\omega_3^2+\omega_4^2)C\psi S\phi + k_M((\omega_2^2-\omega_4^2)C\theta + (\omega_1^2-\omega_3^2)S\theta S\phi)S\psi \\
&+ C\phi(k_M(\omega_1^2-\omega_3^2)C\psi + k_F(\omega_1^2+\omega_2^2+\omega_3^2+\omega_4^2)S\theta S\psi)) \\
&+ C\alpha(C\beta(k_M(-\omega_2^2+\omega_4^2)S\theta + C\theta(k_F(\omega_1^2+\omega_2^2+\omega_3^2+\omega_4^2)C\phi + k_M(\omega_1^2-\omega_3^2)S\phi)) \\
&- S\beta(k_M(\omega_2^2-\omega_4^2)C\theta C\psi + C\phi(k_F(\omega_1^2+\omega_2^2+\omega_3^2+\omega_4^2)C\psi S\theta + k_M(-\omega_1^2+\omega_3^2)S\psi) \\
&+ S\phi(k_M(\omega_1^2-\omega_3^2)C\psi S\theta + k_F(\omega_1^2+\omega_2^2+\omega_3^2+\omega_4^2)S\psi))))\\
Q_5 =& L_rS\alpha(-S\beta(k_M(-\omega_2^2+\omega_4^2)S\theta + C\theta(k_F(\omega_1^2+\omega_2^2+\omega_3^2+\omega_4^2)C\phi \\
&+ k_M(\omega_1^2-\omega_3^2)S\phi)) - C\beta(k_M(\omega_2^2-\omega_4^2)C\theta C\psi + C\phi(k_F(\omega_1^2+\omega_2^2+\omega_3^2+\omega_4^2)C\psi S\theta \\
&+ k_M(-\omega_1^2+\omega_3^2)S\psi) + S\phi(k_M(\omega_1^2-\omega_3^2)C\psi S\theta + k_F(\omega_1^2+\omega_2^2+\omega_3^2+\omega_4^2)S\psi)))\\
Q_6 =& k_FL_Q(\omega_2^2-\omega_4^2)\\
Q_7 =& L_Q(-k_F(\omega_1^2-\omega_3^2)C\phi + k_M(-\omega_1^2+\omega_2^2-\omega_3^2+\omega_4^2)S\phi)\\
Q_8 =& L_Q(k_F(-\omega_2^2+\omega_4^2)S\theta + C\theta(k_M(\omega_1^2-\omega_2^2+\omega_3^2-\omega_4^2)C\phi + k_F(-\omega_1^2+\omega_3^2)S\phi))
\end{aligned}
\tag{A.1}
$$

Matrix M:

$$
\boldsymbol{M} = \begin{bmatrix} \boldsymbol{M}_{11} & \boldsymbol{0}_{5\times3} \\ \boldsymbol{0}_{3\times5} & \boldsymbol{M}_{22} \end{bmatrix} \tag{A.2}
$$

where, $\boldsymbol{M}_{11}$ and $\boldsymbol{M}_{22}$ are defined as follows:

$$
\boldsymbol{M}_{11} = \begin{bmatrix}
m_P+m_Q & 0 & 0 & 0 & -L_rm_QC\beta \\
0 & m_P+m_Q & 0 & L_rm_QC\beta S\alpha & L_rm_QC\alpha S\beta \\
0 & 0 & m_P+m_Q & L_rm_QC\alpha C\beta & -L_rm_QS\alpha S\beta \\
0 & L_rm_QC\beta S\alpha & L_rm_QC\alpha C\beta & L_r^2m_QC\beta^2 & 0 \\
-L_rm_QC\beta & L_rm_QC\alpha S\beta & -L_rm_QS\alpha S\beta & 0 & L_r^2m_Q
\end{bmatrix}
$$

$$
\boldsymbol{M}_{22} = \begin{bmatrix}
I_x & 0 & -I_xS\theta \\
0 & I_yC^2\phi + I_zS^2\phi & (I_y-I_z)C\theta C\phi S\phi \\
-I_xS\theta & (I_y-I_z)C\theta C\phi S\phi & I_xS^2\theta + C^2\theta(I_zC^2\phi + I_yS^2\phi)
\end{bmatrix}
$$

Definitions of function $f(\boldsymbol{q}, \dot{\boldsymbol{q}})$:

$$
\begin{aligned}
f_1(q,\dot{q}) =& k_M\omega_2^2C[\theta]C[\psi] - k_M\omega_4^2C[\theta]C[\psi] + k_F\omega_1^2C[\phi]C[\psi]S[\theta] + k_F\omega_2^2C[\phi]C[\psi]S[\theta] \\
&+ k_F\omega_3^2C[\phi]C[\psi]S[\theta] + k_F\omega_4^2C[\phi]C[\psi]S[\theta] + k_M\omega_1^2C[\psi]S[\theta]S[\phi] \\
&- k_M\omega_3^2C[\psi]S[\theta]S[\phi] - k_M\omega_1^2C[\phi]S[\psi] + k_M\omega_3^2C[\phi]S[\psi] + k_F\omega_1^2S[\phi]S[\psi] \\
&+ k_F\omega_2^2S[\phi]S[\psi] + k_F\omega_3^2S[\phi]S[\psi] + k_F\omega_4^2S[\phi]S[\psi] - L_rm_QS[\alpha]S[\beta]\dot{\alpha}^2 \\
&+ 2L_rm_QC[\alpha]C[\beta]\dot{\alpha}\dot{\beta} - L_rm_QS[\alpha]S[\beta]\dot{\beta}^2 \\
f_2(q,\dot{q}) =& -k_F\omega_1^2C[\psi]S[\phi] - k_F\omega_2^2C[\psi]S[\phi] - k_F\omega_3^2C[\psi]S[\phi] - k_F\omega_4^2C[\psi]S[\phi] \\
&+ k_M\omega_2^2C[\theta]S[\psi] - k_M\omega_4^2C[\theta]S[\psi] + k_M\omega_1^2S[\theta]S[\phi]S[\psi] - k_M\omega_3^2S[\theta]S[\phi]S[\psi] \\
&+ C[\phi](k_M(\omega_1^2-\omega_3^2)C[\psi] + k_F(\omega_1^2+\omega_2^2+\omega_3^2+\omega_4^2)S[\theta]S[\psi]) - L_rm_QC[\alpha]\dot{\alpha}^2 \\
f_3(q,\dot{q}) =& -gm_P - gm_Q + k_F\omega_1^2C[\theta]C[\phi] + k_F\omega_2^2C[\theta]C[\phi] + k_F\omega_3^2C[\theta]C[\phi] \\
&+ k_F\omega_4^2C[\theta]C[\phi] - k_M\omega_2^2S[\theta] + k_M\omega_4^2S[\theta] + k_M\omega_1^2C[\theta]S[\phi] - k_M\omega_3^2C[\theta]S[\phi] \\
&+ L_rm_QC[\beta]S[\alpha]\dot{\alpha}^2 + 2L_rm_QC[\alpha]S[\beta]\dot{\alpha}\dot{\beta} + L_rm_QC[\beta]S[\alpha]\dot{\beta}^2 \\
f_4(q,\dot{q}) =& L_r(S[\alpha](-k_F(\omega_1^2+\omega_2^2+\omega_3^2+\omega_4^2)C[\psi]S[\phi] + k_M((\omega_2^2-\omega_4^2)C[\theta] \\
&+ (\omega_1^2-\omega_3^2)S[\theta]S[\phi])S[\psi] + C[\phi](k_M(\omega_1^2-\omega_3^2)C[\psi] \\
&+ k_F(\omega_1^2+\omega_2^2+\omega_3^2+\omega_4^2)S[\theta]S[\psi])) - C[\alpha](C[\beta](gm_Q + k_M(\omega_2^2-\omega_4^2)S[\theta] \\
&- C[\theta](k_F(\omega_1^2+\omega_2^2+\omega_3^2+\omega_4^2)C[\phi] + k_M(\omega_1^2-\omega_3^2)S[\phi])) \\
&+ S[\beta](k_M(\omega_2^2-\omega_4^2)C[\theta]C[\psi] + C[\phi](k_F(\omega_1^2+\omega_2^2+\omega_3^2+\omega_4^2)C[\psi]S[\theta] \\
&+ k_M(-\omega_1^2+\omega_3^2)S[\psi]) + S[\phi](k_M(\omega_1^2-\omega_3^2)C[\psi]S[\theta] \\
&+ k_F(\omega_1^2+\omega_2^2+\omega_3^2+\omega_4^2)S[\psi])))) + L_rm_QC[\alpha]S[\alpha]\dot{\beta}^2) \\
f_5(q,\dot{q}) =& -L_rS[\alpha](S[\beta](-gm_Q - k_M(\omega_2^2-\omega_4^2)S[\theta] + C[\theta](k_F(\omega_1^2+\omega_2^2+\omega_3^2+\omega_4^2)C[\phi] \\
&+ k_M(\omega_1^2-\omega_3^2)S[\phi])) + C[\beta](k_M(\omega_2^2-\omega_4^2)C[\theta]C[\psi] \\
&+ C[\phi](k_F(\omega_1^2+\omega_2^2+\omega_3^2+\omega_4^2)C[\psi]S[\theta] + k_M(-\omega_1^2+\omega_3^2)S[\psi]) \\
&+ S[\phi](k_M(\omega_1^2-\omega_3^2)C[\psi]S[\theta] + k_F(\omega_1^2+\omega_2^2+\omega_3^2+\omega_4^2)S[\psi])) + 2L_rm_QC[\alpha]\dot{\alpha}\dot{\beta}) \\
f_6(q,\dot{q}) =& \frac{1}{2}(2k_FL_Q(\omega_2^2-\omega_4^2) - (\mathrm{Iyy}-\mathrm{Izz})S[2\phi]\dot{\theta}^2 + 2C[\theta](\mathrm{Ixx} \\
&+ (\mathrm{Iyy}-\mathrm{Izz})C[2\phi])\dot{\theta}\dot{\psi} + (\mathrm{Iyy}-\mathrm{Izz})C[\theta]^2S[2\phi]\dot{\psi}^2) \\
f_7(q,\dot{q}) =& \frac{1}{8}(-8k_FL_Q\omega_1^2C[\phi] + 8k_FL_Q\omega_3^2C[\phi] - 8k_ML_Q\omega_1^2S[\phi] + 8k_ML_Q\omega_2^2S[\phi] \\
&- 8k_ML_Q\omega_3^2S[\phi] + 8k_ML_Q\omega_4^2S[\phi] + 8(\mathrm{Iyy}-\mathrm{Izz})S[2\phi]\dot{\theta}\dot{\phi} \\
&- 8C[\theta](\mathrm{Ixx} + (\mathrm{Iyy}-\mathrm{Izz})C[2\phi])\dot{\phi}\dot{\psi} + 4\mathrm{Ixx}S[2\theta]\dot{\psi}^2 - 2\mathrm{Iyy}S[2\theta]\dot{\psi}^2 - 2\mathrm{Izz}S[2\theta]\dot{\psi}^2 \\
&+ \mathrm{Iyy}S[2(\theta-\phi)]\dot{\psi}^2 - \mathrm{Izz}S[2(\theta-\phi)]\dot{\psi}^2 + \mathrm{Iyy}S[2(\theta+\phi)]\dot{\psi}^2 - \mathrm{Izz}S[2(\theta+\phi)]\dot{\psi}^2) \\
f_8(q,\dot{q}) =& L_Q(k_F(-\omega_2^2+\omega_4^2)S[\theta] + C[\theta](k_M(\omega_1^2-\omega_2^2+\omega_3^2-\omega_4^2)C[\phi] \\
&+ k_F(-\omega_1^2+\omega_3^2)S[\phi])) + (\mathrm{Iyy}-\mathrm{Izz})C[\phi]S[\theta]S[\phi]\dot{\theta}^2 \\
&- (\mathrm{Iyy}-\mathrm{Izz})C[\theta]^2S[2\phi]\dot{\phi}\dot{\psi} + C[\theta]\dot{\theta}((\mathrm{Ixx} + (-\mathrm{Iyy}+\mathrm{Izz})C[2\phi])\dot{\phi} \\
&+ (-2\mathrm{Ixx} + \mathrm{Iyy} + \mathrm{Izz} + (-\mathrm{Iyy}+\mathrm{Izz})C[2\phi])S[\theta]\dot{\psi})
\end{aligned}
\tag{A.3}
$$

Linearized model:

$$
\boldsymbol{A} = \begin{pmatrix}
0 & 1.0 & 0 & 0 & 0 & 0 & 0 & 0 & 0 & 0 & 0 & 0 & 0 & 0 & 0 & 0 \\
0 & 0 & 0 & 0 & 0 & 0 & 0 & 0 & 0 & -9.8 & 0 & 0 & 0 & $-2.6\cdot10^{-15}$ & 0 & 0 & 0 \\
0 & 0 & 0 & 1.0 & 0 & 0 & 0 & 0 & 0 & 0 & 0 & 0 & 0 & 0 & 0 & 0 & 0 \\
0 & 0 & 0 & 0 & 0 & 0 & 0 & 9.8 & 0 & 0 & 0 & $4.3\cdot10^{-15}$ & 0 & 0 & 0 & 0 & 0 \\
0 & 0 & 0 & 0 & 0 & 1.0 & 0 & 0 & 0 & 0 & 0 & 0 & 0 & 0 & 0 & 0 & 0 \\
0 & 0 & 0 & 0 & 0 & 0 & $6.0\cdot10^{-16}$ & 0 & 0 & 0 & $6.0\cdot10^{-16}$ & 0 & 0 & 0 & 0 & 0 & 0 \\
0 & 0 & 0 & 0 & 0 & 0 & 0 & 1.0 & 0 & 0 & 0 & 0 & 0 & 0 & 0 & 0 & 0 \\
0 & 0 & 0 & 0 & 0 & 0 & -21.0 & 0 & 0 & 0 & -21.0 & 0 & 0 & 0 & 0 & 0 & 0 \\
0 & 0 & 0 & 0 & 0 & 0 & 0 & 0 & 0 & 1.0 & 0 & 0 & 0 & 0 & 0 & 0 & 0 \\
0 & 0 & 0 & 0 & 0 & 0 & 0 & 0 & -21.0 & 0 & 0 & 0 & -21.0 & 0 & 0 & 0 & 0 \\
0 & 0 & 0 & 0 & 0 & 0 & 0 & 0 & 0 & 0 & 0 & 1.0 & 0 & 0 & 0 & 0 & 0 \\
0 & 0 & 0 & 0 & 0 & 0 & 0 & 0 & 0 & 0 & 0 & 0 & 0 & 0 & 1.0 & 0 & 0 \\
0 & 0 & 0 & 0 & 0 & 0 & 0 & 0 & 0 & 0 & 0 & 0 & 0 & 0 & 0 & 0 & 0 \\
0 & 0 & 0 & 0 & 0 & 0 & 0 & 0 & 0 & 0 & 0 & 0 & 0 & 0 & 0 & 0 & 1.0 \\
0 & 0 & 0 & 0 & 0 & 0 & 0 & 0 & 0 & 0 & 0 & 0 & 0 & 0 & 0 & 0 & 0
\end{pmatrix}
\tag{A.4}
$$

$$
\boldsymbol{B} = \begin{pmatrix}
0 & 0 & 0 & 0 \\
0 & $-1.7\cdot10^{-19}$ & 0 & $1.7\cdot10^{-19}$ \\
0 & 0 & 0 & 0 \\
$-7.1\cdot10^{-19}$ & $-4.3\cdot10^{-19}$ & $-1.9\cdot10^{-19}$ & $-4.3\cdot10^{-19}$ \\
0 & 0 & 0 & 0 \\
$7.0\cdot10^{-3}$ & $7.0\cdot10^{-3}$ & $7.0\cdot10^{-3}$ & $7.0\cdot10^{-3}$ \\
0 & 0 & 0 & 0 \\
$5.8\cdot10^{-4}$ & $9.3\cdot10^{-19}$ & $-5.8\cdot10^{-4}$ & $9.3\cdot10^{-19}$ \\
0 & 0 & 0 & 0 \\
0 & $-5.8\cdot10^{-4}$ & 0 & $5.8\cdot10^{-4}$ \\
0 & 0 & 0 & 0 \\
0 & 0.31 & 0 & -0.31 \\
0 & 0 & 0 & 0 \\
-0.25 & 0 & 0.25 & 0 \\
0 & 0 & 0 & 0 \\
$5.9\cdot10^{-3}$ & $-5.9\cdot10^{-3}$ & $5.9\cdot10^{-3}$ & $-5.9\cdot10^{-3}$
\end{pmatrix}
\tag{A.5}
$$